ORIGINAL RESEARCH

Ultraviolet B Exposure Inhibits Angiotensin II–Induced Abdominal Aortic Aneurysm Formation in Mice by Expanding $CD4^+Foxp3^+$ Regulatory T Cells

Tomohiro Hayashi, MD; Naoto Sasaki, MD, PhD; Tomoya Yamashita, MD, PhD; Taiji Mizoguchi, MD, PhD; Takuo Emoto, MD, PhD; Hilman Zulkifli Amin, MD; Keiko Yodoi, MD, PhD; Takuya Matsumoto, MD, PhD; Kazuyuki Kasahara, MD, PhD; Naofumi Yoshida, MD; Tokiko Tabata, MD; Naoki Kitano, MS; Atsushi Fukunaga, MD, PhD; Chikako Nishigori, MD, PhD; Yoshiyuki Rikitake, MD, PhD; Ken-ichi Hirata, MD, PhD

***Background*—**Pathogenic immune responses are known to play an important role in abdominal aortic aneurysm (AAA) development. Ultraviolet B (UVB) irradiation has been demonstrated to have therapeutic potential not only for cutaneous diseases but also for systemic inflammatory diseases in mice by suppressing immunoinflammatory responses. We investigated the effect of UVB irradiation on experimental AAA.

***Methods and Results*—**We used an angiotensin II–induced AAA model in apolipoprotein E–deficient mice fed a high-cholesterol diet. Mice aged 10 weeks were irradiated with 5 kJ/m^2 UVB once weekly for 6 weeks (UVB-irradiated, n=38; nonirradiated, n=42) and were euthanized for evaluation of AAA formation at 16 weeks. Overall, 93% of angiotensin II–infused mice developed AAA, with 60% mortality possibly because of aneurysm rupture. UVB irradiation significantly decreased the incidence (66%) and mortality (29%) of AAA (P=0.004 and P=0.006, respectively). UVB-irradiated mice had significantly smaller diameter AAA (P=0.008) and fewer inflammatory cells in the aortic aneurysm tissue than nonirradiated mice, along with systemic expansion of $CD4^+Foxp3^+$ regulatory T cells and decreased effector $CD4^+CD44^{high}CD62L^{low}$ T cells in para-aortic lymph nodes. Genetic depletion of regulatory T cells abrogated these beneficial effects of UVB treatment, demonstrating a critical role of regulatory T cells.

***Conclusions*—**Our data suggest that UVB-dependent expansion of regulatory T cells has beneficial effects on experimental AAA and may provide a novel strategy for the treatment of AAA. **(*J Am Heart Assoc*. 2017;6:e007024. DOI: 10.1161/JAHA.117.007024.)**

Key Words: abdominal aortic aneurysm • immunology • inflammation

Abdominal aortic aneurysm (AAA), which is characterized by dilation of the abdominal aorta, is a major potentially lethal aortic disease in developed countries.[1,2] AAA is often asymptomatic until the time of rupture and has up to a 90% risk of death if the aneurysm ruptures. Despite similar lifestyle-associated risk factors for AAA and coronary heart disease, pharmacological treatment for such risk factors has little beneficial effect on aneurysm growth and rupture.[3] Because surgical treatment is not recommended until the risk of rupture exceeds that of interventional procedure, management of patients is a matter of observation until the diameter of the aorta runs up to a size at which surgery is indicated. Consequently, it is important to explore the pathophysiology of AAA formation and to develop a noninvasive therapeutic approach to preventing AAA.

Immunoinflammatory responses in the vessel wall have been shown to be a key feature shared by AAA and atherosclerotic disease. Recent experimental evidence has

From the Division of Cardiovascular Medicine, Department of Internal Medicine (T.H., N.S., T.Y., T. Mizoguchi, T.E., H.Z.A., K.Y., T. Matsumoto, K.K., N.Y., T.T., N.K., K.-i.H.) and Division of Dermatology, Department of Internal Related (A.F., C.N.), Kobe University Graduate School of Medicine, Kobe, Japan; Department of Medical Pharmaceutics, Kobe Pharmaceutical University, Kobe, Japan (N.S., H.Z.A., Y.R.); Department of Internal Medicine, Faculty of Medicine, Universitas Indonesia, Jakarta, Indonesia (H.Z.A.).

Accompanying Figures S1 through S5 are available at http://jaha.ahajournals.org/content/6/9/e007024/DC1/embed/inline-supplementary-material-1.pdf

Correspondence to: Naoto Sasaki, MD, PhD, Department of Medical Pharmaceutics, Kobe Pharmaceutical University, 4-19-1, Motoyamakita-machi, Higashinada-ku, Kobe 658-8558, Japan. E-mail: n-sasaki@kobepharma-u.ac.jp

Received June 25, 2017; accepted July 25, 2017.

Clinical Perspective

What Is New?

- Ultraviolet B (UVB) irradiation inhibited the development of angiotensin II–induced abdominal aortic aneurysm and reduced mortality under hypercholesterolemic conditions.
- The protective effects of UVB therapy were associated with systemic expansion of immunosuppressive $CD4^+Foxp3^+$ regulatory T cells and reduced inflammatory responses in the aortic aneurysm tissue.
- Experimental studies in regulatory T cell–depleted mice clearly demonstrated that UVB-induced $CD4^+Foxp3^+$ regulatory T cells played a critical role in limiting aortic inflammation and abdominal aortic aneurysm development.

What Are the Clinical Implications?

- In clinical settings, appropriately conducted UVB-based phototherapy is safe and effective for immunoinflammatory cutaneous disorders such as psoriasis and atopic dermatitis.
- Although our findings should be cautiously applied to clinical practice, our data suggest that UVB-mediated modulation of immunoinflammatory reactions could be an attractive noninvasive approach to preventing abdominal aortic aneurysm.

indicated that immune cells such as T cells and macrophages are the predominant inflammatory cells and play a key role in causing chronic inflammation in the aortic wall, which contributes to the development of atherosclerosis and AAA.[4] Similar to the situation of atherosclerotic disease, effector T cell–mediated (Teff-mediated) immune responses are responsible for the development of AAA, although there are some differences in regulation.[5] A shift toward a T helper type 2 (Th2) immune response is reported to be critical for AAA formation in mice and humans,[6,7] whereas a Th1 immune response promotes atherosclerosis.[8] An important report showed that promotion of Th1 immune responses prevents AAA but has adverse effects on atherosclerotic disease.[9] In contrast to these reports, a Th1 immune response has been shown to contribute to the development of AAA in mice[10] and humans.[11] Consequently, the role of each helper T-cell subset in AAA remains controversial. Compelling data suggest that regulatory T cells (Tregs) expressing a CD25 (interleukin 2 [IL-2] receptor α-chain) molecule and Foxp3 (forkhead box P3), known to suppress pathogenic immune responses, play a critical role in inhibiting the development and progression of atherosclerosis[12–14] and angiotensin II–induced AAA formation[15–18] by dampening Teff immune responses in mice. A recent clinical report showed that patients with AAA have markedly decreased numbers of peripheral $CD4^+CD25^+Foxp3^+$ Tregs and functional deficiency compared with healthy control participants.[19] Another study demonstrated that Foxp3 expression levels in peripheral blood cells correlate significantly negatively with AAA annual growth rates.[18] These reports suggest that impaired Treg-mediated immunoregulation might be closely related to AAA formation. Considering that patients with AAA have high incidence of atherosclerotic disease, we expect that therapeutic intervention aimed at enhancing a Treg-mediated immune response could be a valuable therapeutic approach to preventing AAA under atherosclerotic conditions. We and others recently showed that injection of a recombinant mouse IL-2/anti–IL-2 monoclonal antibody complex selectively expands $CD4^+Foxp3^+$ Tregs and effectively inhibits atherosclerosis[20] and angiotensin II–induced AAA formation[17] in apolipoprotein E–deficient ($Apoe^{-/-}$) mice. Nevertheless, despite the efficacy and safety of pharmacological therapies using antibodies and cytokines in experimental studies, those therapies may cause severe adverse effects such as activation of excessive immune responses in humans and thus cannot be easily applied to clinical situations.

Ultraviolet irradiation, in particular, the midwavelength range (ultraviolet B [UVB]), is known to have many biological effects on the immune system.[21] UVB irradiation has been shown to suppress cutaneous and systemic inflammatory diseases by modulating Teff immune responses, which may vary depending on the disease models used.[22–24] We recently investigated the effect of UVB irradiation on atherosclerosis in hypercholesterolemic mice and demonstrated that UVB exposure prevents atherosclerosis by expanding activated $CD4^+Foxp3^+$ Tregs and by suppressing pathogenic immune responses.[25] Importantly, in clinical settings, immunoinflammatory cutaneous disorders such as psoriasis are treated with UVB without any serious side effects. These data imply that UVB-dependent regulation of pathogenic inflammatory responses could be a possible approach to preventing AAA under atherosclerotic conditions. If so, this therapy could be clinically applicable for treating AAA.

In this study, we investigated the effect of UVB irradiation on the development of AAA and its underlying mechanisms in angiotensin II–infused $Apoe^{-/-}$ mice. Moreover, using hypercholesterolemic Treg-depleted mice, we explored the contribution of $CD4^+Foxp3^+$ Tregs to AAA development following UVB exposure.

Methods

Animals and Experimental Design

All mice were on a C57BL/6 background, and $Apoe^{-/-}$ mice are maintained in an animal facility at Kobe University.[26] In total, 220 mice were used in this study. Six-week-old male mice were fed a high-cholesterol diet containing 0.2%

cholesterol and 21% fat and water ad libitum. At 12 weeks of age, mice were infused with angiotensin II (1000 ng/kg per minute) or normal saline (sham group) for 7 or 28 days by implanting ALZET miniosmotic pumps (model 2004; DURECT Corp), as described previously.[27] To study the effect of UVB irradiation on the development of AAA, 10-week-old *Apoe*$^{-/-}$ mice were irradiated with 5 kJ/m^2 UVB once weekly for 6 weeks. Nonirradiated mice served as controls. For in vivo selective depletion of CD4$^+$Foxp3$^+$ Tregs, we used DEREG (depletion of Tregs) mice on an *Apoe*$^{-/-}$ background (DEREG/*Apoe*$^{-/-}$ mice), as described previously.[17] To deplete CD4$^+$Foxp3$^+$ Tregs, DEREG/*Apoe*$^{-/-}$ mice were injected with 1.0 μg diphtheria toxin diluted in endotoxin-free PBS for 2 consecutive days before implantation of ALZET miniosmotic pumps and once weekly thereafter for 4 weeks. We produced angiotensin II–induced AAA in DEREG/*Apoe*$^{-/-}$ mice under the same protocol described. Mice were euthanized at 16 weeks of age for evaluation of AAA formation. We housed mice in a specific pathogen-free animal facility at Kobe University, and all animal experiments were conducted according to the guidelines for animal experiments at Kobe University School of Medicine.

UVB Irradiation

TL 20W/12RS fluorescent lamps (Philips) were used to irradiate the mice with broadband UVB. TL 20W/12RS lamps emit a continuous spectrum from 275 to 390 nm, with peak emission at 313 nm; ≈65% of that radiation is within the UVB wavelength range (280–320 nm). The irradiance was 6.6 J/m^2 per second at a distance of 40 cm, as measured by a UIT-250 digital UV intensity meter (USHIO). The mice were placed 40 cm below the bank of lamps and irradiated at the indicated weeks after their backs were shaved, as described previously.[28]

Blood Pressure Measurement

Systolic blood pressure (SBP) was measured by the noninvasive tail-cuff method, as described previously.[29] SBP was measured at least 5 times at baseline and 4 weeks after angiotensin II pump implantation. The mean SBP for each group was determined by averaging the SBP of each mouse included in that group.

Assessment of Biochemical Parameters

After overnight fasting, blood was collected by cardiac puncture under anesthesia. Plasma was obtained through centrifugation and stored at −80°C until measurement. Concentrations of plasma total cholesterol, high-density lipoprotein cholesterol, and triglyceride were determined enzymatically using an automated chemistry analyzer. In addition, 1,25-dihydroxyvitamin D and 25-hydroxyvitamin D were analyzed by radioimmunoassay, as described previously.[30]

Morphological Analysis of AAA

Aortic diameters and AAA incidence were determined, as described previously.[27] For morphological analyses, aortas were perfused with normal saline and fixed in 10% buffered formalin. The maximum external aortic diameters were measured using ImageJ (National Institutes of Health). Aneurysm incidence was quantified on the basis of a definition of an external suprarenal aorta width that was increased by ≥50% compared with saline-infused mice. We used a previously described classification system[17] to categorize the morphological severity of the aneurysms: no aneurysm; type I, a discernable dilation that is 1.5–2 times the diameter of a normal abdominal aorta; type II, a single large dilation >2 times the diameter of a normal abdominal aorta; type III, multiple dilations generally extending proximal to the suprarenal region; type IV, death caused by aneurysmal rupture.

Histological and Immunohistochemical Analysis of Aneurysmal Lesions

Mice were anesthetized, and the aorta was perfused with saline. The AAA lesions were cut and embedded in OCT compounds, and cross-sections (10 μm) were prepared. For the determination of elastin degradation, we performed Elastica van Gieson staining and used a standard score for the grades of elastin degradation, as described previously.[17] Three sections were analyzed in each mouse, and grading score was determined by calculating the average grade of the sections. The grades were defined as follows: grade 1, no degradation; grade 2, mild elastin degradation; grade 3, severe elastin degradation; grade 4, aortic rupture. Immunohistochemistry was performed on acetone- or formalin-fixed cryosections (10 μm) of mouse AAA lesions using antibodies to identify macrophages (MOMA-2, 1:400), T cells (CD4, 1:100), and Foxp3$^+$ Tregs (Foxp3, clone FJK-16s, 1:100; eBioscience), followed by detection with biotinylated secondary antibodies and streptavidin–horseradish peroxidase. The appropriate fixation reagent, depending on the primary antibodies, was used. Stained sections were observed under an All-in-one–type fluorescence microscope (BZ-X700; Keyence) using the BZ Analyzer software (Keyence). Stained sections were digitally captured, and the stained area was calculated. Four consecutive sections of AAA lesions with the maximum size were analyzed in each mouse, and the average values were used for statistical analysis. Quantitative analyses

of $CD4^+$ T cells and $Foxp3^+$ cells of the AAA lesions were performed by counting the positively stained cells, which were divided by the total area of each cross-section.

Flow Cytometry

For fluorescence-activated cell sorter analysis of lymphoid tissues, peripheral (inguinal and axillary) lymph node (LN) cells and splenocytes were isolated and stained in PBS containing 2% fetal calf serum. Flow cytometric analysis was performed with the Attune acoustic focusing cytometer (Life Technologies) using FlowJo software (Tree Star). For intracellular cytokine staining, splenocytes were stimulated with 20 ng/mL phorbol 12-myristate 13-acetate and 1 mmol/L ionomycin for 5 hours in the presence of GolgiStop (BD Biosciences). After staining for surface antigens, intracellular cytokine staining was performed using an intracellular cytokine staining kit and anti-cytokine antibodies, according to the manufacturer's instructions (BD Biosciences). The antibodies used were as follows: anti-CD4 FITC (clone H129.19; BD Biosciences), anti-CD4 APCcy7 (clone GK1.5; BD Biosciences), anti-CD25 (clone PC61; BD Biosciences), anti-CD44 (clone IM7; BD Biosciences), anti-CD62L (clone MEL-14; BD Biosciences), anti-CD103 (clone M290; BD Biosciences), anti-GITR (anti–glucocorticoid-induced tumor necrosis factor receptor family-related gene/protein; clone DTA1; BD Biosciences), anti–CTLA-4 (anti–cytotoxic T lymphocyte-associated antigen 4; clone UC10; BD Biosciences), anti-Foxp3 (clone FJK-16s; eBioscience), anti-CD11b (clone M1/70; BD Biosciences), anti-CD11c (clone HL3; BD Biosciences), anti-CD80 (clone 16-10A1; BD Biosciences), anti-CD86 (clone GL1; BD Biosciences), anti-Ly6C (clone AL-21; BD Biosciences), anti-Ly6G (clone 1A8; BD Biosciences), anti–IL-4 (clone BVD4-1D11; eBioscience), anti–IL-10 (clone JES5-16E3; eBioscience), anti–IL-17 (clone 17-B7; BD Bioscience), anti–INF-y (anti–interferon γ; clone XMG1.2; eBioscience), and isotype-matched control antibodies. Intracellular staining of Foxp3 was performed using the Foxp3 staining buffer set (eBioscience), according to the manufacturer's instructions. All staining procedures were performed after blocking the fold-chain receptor with anti-CD16/CD32 (clone 2.4G2; BD Bioscience). Surface stainings were performed according to standard procedures at a density of 5 to 10×10^5 cells per 50 μL, and volumes were scaled up accordingly.

Real-Time Reverse Transcription Polymerase Chain Reaction Analysis

Total RNA was extracted from suprarenal aortas after perfusion with RNAlater (Life Technologies) using TRIzol reagent (Life Technologies). For reverse transcription, a PrimeScript reverse transcription reagent kit (Takara) was used. Quantitative polymerase chain reaction was performed, as described previously, using a SYBR Premix Ex Taq (Takara) and an ABI PRISM 7500 sequence detection system (Life Technologies), according to the manufacturers' protocols. The following primers were used to amplify IFN-γ, IL-6, TNF-α (tumor necrosis factor α), MMP-2 (matrix metalloproteinase 2), MMP-9, Foxp3, CTLA-4, CD25, and GAPDH: IFN-γ, 5′-CGG CAC AGT CAT TGA AAG CCT A-3′ and 5′-GTT GCT GAT GGC CTG ATT GCT-3′; IL-6, 5′-CCA CTT CAC AAG TCG GAG GCT TTA-3′ and 5′-GCA AGT GCA TCA TCG TTG TTC ATA C-3′; TNF-α, 5′-AAA CTG GTC GGG CAA TTC TG-3′ and 5′-AGG GTT GGA CAC CTG AAT GCT A-3′; MMP-2, 5′-GAT AAC CTG GAT GCC GTC GTG-3′ and 5′-CTT CAC GCT CTT GAG ACT TTG GTT C-3′; MMP-9, 5′-GCC CTG GAA CTC ACA CGA CA-3′ and 5′-TTG GAA ACT CAC ACG CCA GAA G-3′; Foxp3, 5′-CTC ATG ATA GTG CCT GTG TCC TCA A-3′ and 5′-AGG GCC AGC ATA GGT GCA AG-3′; CTLA-4, 5′-CCT CTG CAA GGT GGA ACT CAT GTA-3′ and 5′-AGC TAA CTG CGA CAA GGA TCC AA-3′; CD25, 5′-CTG ATC CCA TGT GCC AGG AA-3′ and 5′-AGG GCT TTG AAT GTG GCA TTG -3′; GAPDH, 5′-TGT GTC CGT CGT GGA TCT GA-3′ and 5′-TTG CTG TTG AAG TCG CAG GAG-3′. Amplification reactions were performed in duplicate, and fluorescence curves were analyzed with included software. GAPDH was used as an endogenous control reference.

Statistical Analysis

SBP data in the same group were compared with a paired *t* test. Data are expressed as mean±SEM for normally distributed variables or as median (25th–75th percentiles) for nonnormally distributed variables and compared between 2 groups using an unpaired *t* test or Mann–Whitney *U* test, respectively. Kaplan–Meier survival curves were constructed and analyzed using a log-rank (Mantel-Cox) test. AAA incidence and mortality were analyzed using the χ^2 test or Fisher exact test, as appropriate. A value of $P<0.05$ was considered statistically significant. For statistical analysis, GraphPad Prism version 6.0 (GraphPad Software) was used.

Results

UVB Irradiation Inhibits the Development of Angiotensin II–Induced AAA and Reduces Mortality in *Apoe*$^{-/-}$ Mice

To investigate the effect of UVB irradiation on the development of AAA, we used an angiotensin II–induced AAA model and treated 12-week-old *Apoe*$^{-/-}$ mice fed a high-cholesterol diet with angiotensin II infusion for 28 days. Ten-week-old *Apoe*$^{-/-}$ mice were irradiated with 5 kJ/m^2 UVB once weekly for 6 weeks and were euthanized at

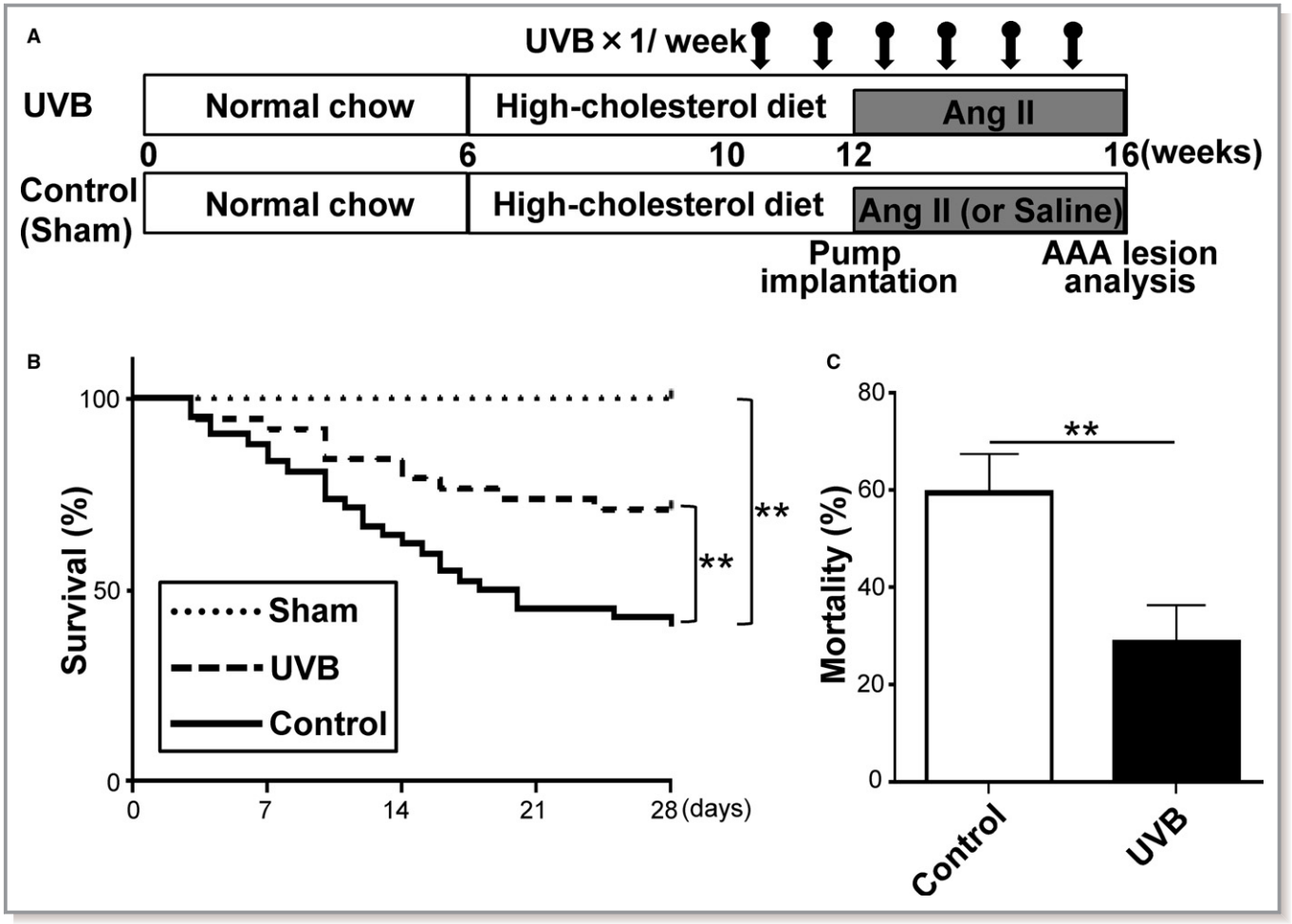

Figure 1. UVB irradiation limits the development of Ang II–induced AAA. A, Experimental design. Arrows represent 5 kJ/m^2 UVB irradiation. Apolipoprotein E-deficient (*Apoe*$^{-/-}$) mice aged 12 weeks and fed a high-cholesterol diet were treated with Ang II infusion for 28 days. Ten-week-old *Apoe*$^{-/-}$ mice were irradiated with 5 kJ/m^2 UVB once weekly for 6 weeks and were euthanized at 16 weeks of age for evaluation of AAA formation. Nonirradiated mice infused with Ang II or saline served as controls or shams, respectively. B, Kaplan–Meier curve shows survival rate in UVB-irradiated (n=38), nonirradiated (n=42), and sham (n=12) mice. C, Mortality due to AAA rupture in UVB-irradiated (n=38) and nonirradiated (n=42) mice. Error bars represent standard error. ***P*<0.01. AAA indicates abdominal aortic aneurysm; Ang II, angiotensin II; UVB, ultraviolet B.

16 weeks of age for evaluation of AAA formation (Figure 1A). We found no severe adverse effects such as skin cancer or skin inflammation following UVB irradiation during the experiments. UVB irradiation did not affect body weight, plasma lipid profile, and plasma levels of biologically active 1,25-dihydroxyvitamin D and circulating storage form 25-hydroxyvitamin D (Table 1). Angiotensin II infusion led to a significant elevation in SBP of UVB-irradiated and nonirradiated mice, whereas there was no significant difference in SBP between the 2 groups (Table 1). Overall, 93% of angiotensin II–infused nonirradiated mice developed AAA with 60% mortality possibly caused by an aneurysm rupture (Figures 1B, 1C, 2A, and 2B). However, a significant decrease in the incidence (66%) and mortality (29%) of AAA was seen on UVB irradiation (Figures 1B, 1C, 2A, and 2B). These results demonstrate the beneficial effects of UVB irradiation on AAA.

UVB Irradiation Suppresses Inflammatory Responses in the Aneurysmal Lesions and Reduces the Severity of Angiotensin II–Induced AAA

In parallel with the evaluation of AAA formation and survival, histological analysis of the aortic aneurysm tissue was performed. Notably, along with a reduction in incidence and mortality (Figures 1B, 1C, and 2B), UVB irradiation decreased the severity of AAA in angiotensin II–infused mice (Figure 2C). UVB-irradiated mice had significantly smaller diameter of the abdominal aneurysm (Figure 2D) and more preserved elastin

Table 1. Body Weight, SBP, Plasma Lipid Profile, and Vitamin D Levels in 16-Week-Old UVB-Irradiated and Nonirradiated Apolipoprotein E–Deficient Mice

Parameters	Control	UVB
Body weight, g	28.3±0.7 (n=17)	29.2±0.5 (n=27)
SBP (before), mm Hg	103.4±1.7 (n=17)	104.5±1.2 (n=27)
SBP (after), mm Hg	132.9±3.3* (n=17)	134.6±2.1* (n=27)
Total cholesterol, mg/dL	949.4±120.2 (n=8)	950.5±55.5 (n=12)
HDL cholesterol, mg/dL	9.0±1.0 (n=8)	9.5±1.4 (n=12)
Triglycerides, mg/dL	26.9±3.1 (n=8)	32.8±5.1 (n=12)
1,25-dihydroxyvitamin D, pg/mL	162.0 (156.0–320.0) (n=6)	185.5 (159.0–243.3) (n=6)
25-hydroxyvitamin D, ng/mL	53.5 (41.0–58.3) (n=6)	46.0 (32.8–53.5) (n=6)

Data are expressed as mean±SEM or median (25–75% quartiles). HDL indicates high-density lipoprotein; SBP, systolic blood pressure; SBP (before), SBP before angiotensin II infusion; SBP (after), SBP after angiotensin II infusion for 4 weeks; UVB, ultraviolet B. *P<0.05 vs SBP (before) in the same group. There are no statistically significant differences in all parameters between UVB-irradiated and nonirradiated mice.

content in the aortic aneurysm tissue than nonirradiated mice (Figure S1A and S1B).

Vascular inflammation is reported to be involved in the mechanisms of angiotensin II–induced AAA development in *Apoe*$^{-/-}$ mice.[27] The aneurysmal lesions consist of lymphocytes infiltration and accumulation of macrophages, which are known to be the main inflammatory cells in this mouse AAA model.[4] To determine the effects of UVB irradiation on CD4$^+$ T cell and macrophage infiltration to the aortic wall, we performed immunohistochemical studies of the aneurysmal lesions in aorta. Notably, the aneurysmal lesions of UVB-irradiated mice showed a marked reduction in the accumulation of macrophages and CD4$^+$ T cells (Figure 3A and 3B) compared with nonirradiated mice. To further examine the effect of UVB irradiation on the accumulation of immunoregulatory Foxp3$^+$ Tregs into aneurysmal lesions, we also performed immunohistochemical analysis using anti-Foxp3 antibody and found that the number of Tregs in the aortic lesions was not significantly changed by UVB irradiation (Figure 3A and 3B). Notably, the Treg/CD4$^+$ T cell ratio within the aneurysmal lesions in UVB-irradiated mice was dramatically increased compared with nonirradiated mice (Figure 3C).

To evaluate the immunoinflammatory responses in aneurysmal tissues following UVB irradiation, we examined mRNA expression of proinflammatory cytokines, MMPs, and Treg-associated molecules in suprarenal aortas by quantitative reverse transcription polymerase chain reaction. Notably, the mRNA expression of proinflammatory cytokine IFN-γ was markedly reduced in UVB-irradiated mice compared with nonirradiated mice (Figure S2A). In addition, the mRNA expression of proinflammatory cytokines (ie, IL-6 and TNF-α) and proteins that degrade extracellular matrix proteins (ie, MMP-2 and MMP-9) tended to be decreased (Figure S2A). Consistent with the results of immunohistochemical analysis showing no changes in the number of Tregs in aneurysmal lesions following UVB irradiation, the mRNA expression of aortic Treg-associated molecules Foxp3, CTLA-4, and CD25 was not significantly changed by UVB irradiation (Figure S2B).

Collectively, these results suggest that UVB irradiation inhibits migration of inflammatory cells into the aneurysmal lesions of angiotensin II–infused mice without affecting the lesional accumulation of Foxp3$^+$ Tregs and subsequently increases the Treg/Teff ratio in the aneurysmal lesions, leading to preserved vessel integrity and decreased susceptibility to AAA and aortic rupture possibly by regulating local inflammatory responses.

UVB Irradiation Expands CD4$^+$Foxp3$^+$ Tregs and Suppresses Pathogenic T-Cell Responses

We next investigated the mechanisms by which UVB irradiation prevents AAA, focusing on the changes in systemic immune responses. We treated 12-week-old *Apoe*$^{-/-}$ mice fed a high-cholesterol diet with angiotensin II infusion for 7 days. Ten-week-old *Apoe*$^{-/-}$ mice were irradiated with 5 kJ/m^2 UVB once weekly for 3 weeks. At 7 days after pump implantation and 4 days after the last UVB irradiation, lymphoid cells from skin-draining LNs and spleen were prepared and analyzed by flow cytometry. Consistent with our previous report using *Apoe*$^{-/-}$ mice without angiotensin II infusion,[25] UVB irradiation significantly increased the frequency of CD4$^+$Foxp3$^+$ Tregs in the skin-draining LNs of angiotensin II–infused mice (Figure 4A). Moreover, an increase in frequency of CD4$^+$Foxp3$^+$ Tregs was also observed in the spleen of UVB-irradiated mice (Figure 4A). CD4$^+$Foxp3$^+$ Tregs from UVB-irradiated mice expressed higher levels of typical Treg markers including CTLA-4, known to be essential for Treg-mediated suppression, and CD103 compared with those from nonirradiated mice (Figure 4B), implying an activated phenotype of CD4$^+$Foxp3$^+$ Tregs following UVB irradiation. There were no differences in the expression of CD25 and GITR between the groups (Figure 4B).

To determine whether UVB irradiation changes T-cell responses, we examined cytokine secretion from CD4$^+$ T cells by intracellular cytokine staining. UVB irradiation did not change the percentage of IFN-γ–producing Th1 cells, IL-4–producing Th2 cells, Th1/Th2 ratio, or IL-17–producing Th17 cells (Figure 4C). UVB irradiation did not affect other splenic immune cell subsets or the expression of maturation markers CD80 and CD86 on splenic CD11c$^+$ dendritic cells (Figure S3). To determine whether UVB irradiation suppresses T-cell activation in vivo, we examined T-cell activation markers of

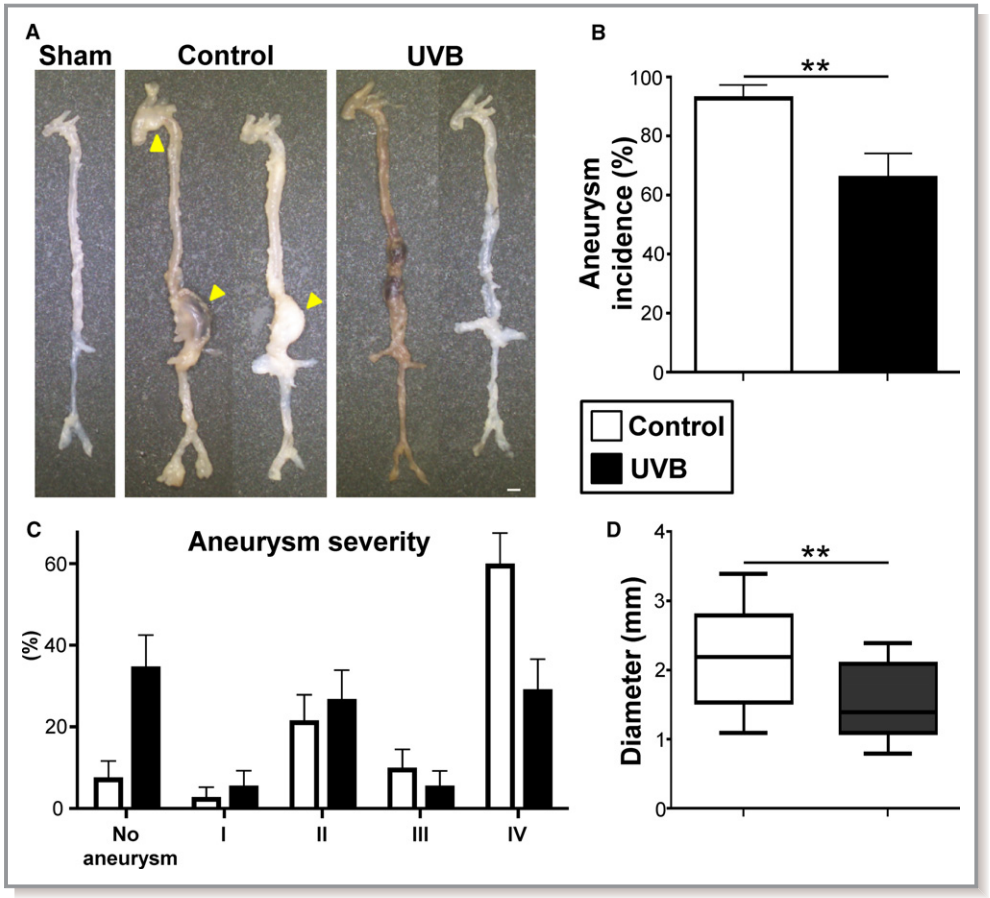

Figure 2. UVB irradiation reduces the severity of Ang II–induced AAA. A, Representative photographs showing macroscopic features of aneurysms induced by Ang II. No animals infused with normal saline developed aneurysm (left specimen). Infusion of Ang II in apolipoprotein E–deficient mice developed AAA (middle and right). Arrowheads indicate abdominal and thoracic aneurysms. Scale bar=1 mm. B, Incidence of AAA in UVB-irradiated (n=38) and nonirradiated (n=42) mice. C, Severity of aneurysm in UVB-irradiated (n=27) and nonirradiated (n=17) mice. Error bars represent standard error in (B and C). D, Maximal diameter of abdominal aorta in UVB-irradiated (n=27) and nonirradiated (n=17) mice. In the box-and-whisker plot, middle line represents median value, box indicates interquartile range (25th–75th percentiles), and range bars show maximum and minimum. $^{**}P<0.01$. AAA indicates abdominal aortic aneurysm; Ang II, angiotensin II; UVB, ultraviolet B.

peripheral LNs and spleen and found that the proportions of $CD44^{high}CD62L^{low}$ $CD4^+$ Teffs in spleen were comparable between UVB-irradiated and nonirradiated mice (Figure S3). Notably, a decrease in the proportion of $CD44^{high}CD62L^{low}$ $CD4^+$ Teffs in the para-aortic LNs of UVB-irradiated mice was observed (Figure 4D), although we found no changes in the frequency of $CD4^+Foxp3^+$ Tregs in the para-aortic LNs following UVB irradiation (data not shown). These results indicate that UVB irradiation expands activated $CD4^+Foxp3^+$ Tregs in skin-draining LNs and spleen and inhibits the accumulation of Teffs in para-aortic LNs and aneurysmal lesions, which may lead to suppression of pathogenic immunoinflammatory responses and AAA development.

Moreover, considering the findings of few numbers of Tregs in the AAA lesions and no effect of UVB irradiation on their migration into the AAA lesions, we suppose that systemic effects of Tregs would be more important for limiting AAA development than their local effects.

UVB-Induced $CD4^+Foxp3^+$ Tregs Play a Critical Role in Limiting AAA Development

To directly investigate the systemic effects of $CD4^+Foxp3^+$ Tregs on the prevention of AAA development following UVB irradiation, we took advantage of a well-validated DEREG mouse model, which expresses a diphtheria toxin receptor–enhanced green fluorescent protein fusion protein under the control of the *Foxp3* gene locus[31] and is shown to be useful for studying the role of $CD4^+Foxp3^+$ Tregs in chronic disease including AAA[17] and atherosclerosis.[13] To address whether

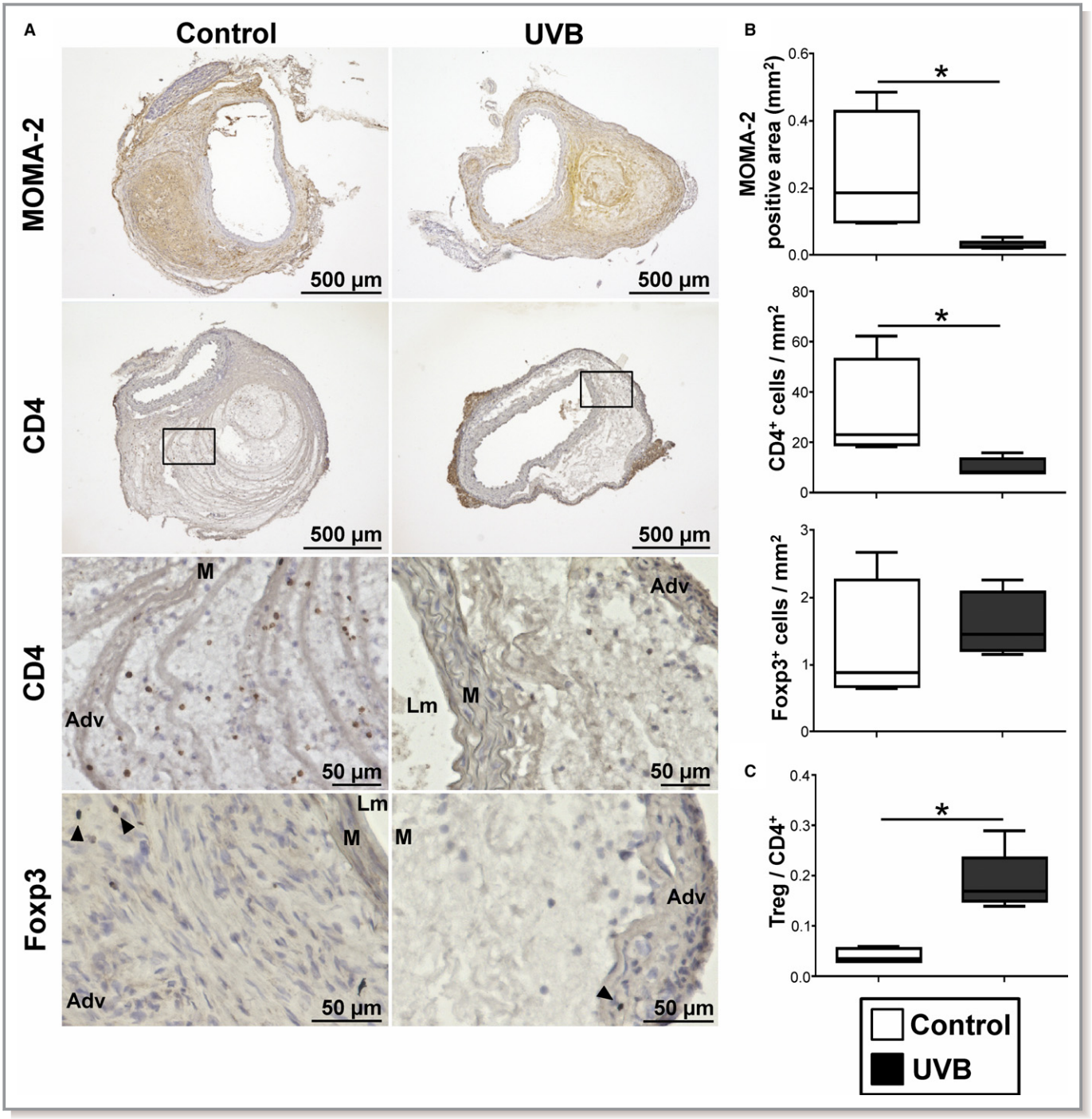

Figure 3. UVB irradiation inhibits effector T cell infiltration and macrophage accumulation in aneurysmal tissues. A, Representative photomicrographs of MOMA-2, CD4, and Foxp3 staining in the abdominal aortic aneurysm lesions of UVB-irradiated and nonirradiated mice. Boxed area is expanded to show representative high-power fields in serial sections. Arrowheads indicate $Foxp3^+$ cells. Scale bar, as shown in figures. B, Quantitative analyses of MOMA-2^+ macrophages, $CD4^+$ T cells, and $Foxp3^+$ regulatory T cells (Tregs) in the aneurysmal lesions in UVB-irradiated (n=5) and nonirradiated (n=4) mice. C, The ratio of $Foxp3^+$ Tregs to $CD4^+$ T cells was determined (Treg/$CD4^+$ T cell ratio). In the box-and-whisker plots shown in (B and C), middle line represents median value, box indicates interquartile range (25th–75th percentiles), and range bars show maximum and minimum. *P<0.05. Adv indicates adventitia; Lm, lumen; M, media; UVB, ultraviolet B.

UVB-expanded $CD4^+Foxp3^+$ Tregs contribute to prevention of AAA development, we used DEREG mice on an *Apoe*$^{-/-}$ background (DEREG/*Apoe*$^{-/-}$ mice).[17] Consistent with previous reports,[17] diphtheria toxin injection in DEREG/*Apoe*$^{-/-}$ mice led to marked depletion of $CD4^+Foxp3^+$ Tregs in the LNs and spleen (Figure S4A). UVB-dependent expansion

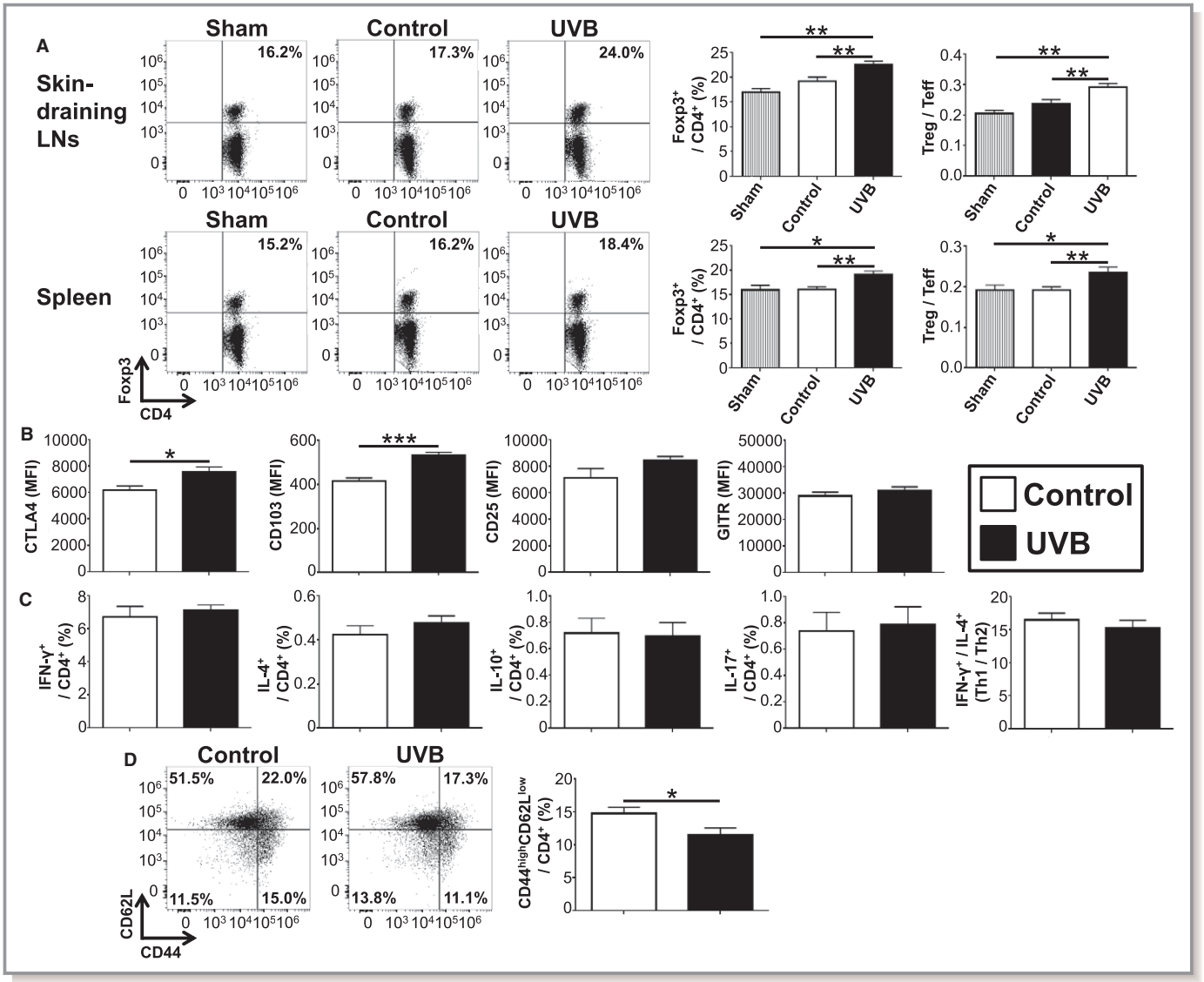

Figure 4. UVB irradiation expands $CD4^+Foxp3^+$ regulatory T cells (Tregs) and suppresses pathogenic T cell responses in angiotensin II–infused mice. Apolipoprotein E–deficient mice were irradiated with 5 kJ/m^2 UVB once weekly for 3 weeks. Nonirradiated mice infused with angiotensin II or saline served as controls or shams, respectively. At 7 days after the pump implantation and 4 days after the last UVB irradiation, lymphoid cells from skin-draining LNs, para-aortic LNs, and spleen were prepared. A, Representative results of Foxp3 expression in skin-draining LN and splenic $CD4^+$ T cells assessed by flow cytometry. The graphs represent the percentage of $Foxp3^+$ Tregs within the LN and spleen $CD4^+$ population. The ratio of $CD4^+Foxp3^+$ Tregs to $CD4^+Foxp3^-$ effector T cells (Teffs) was also determined (Treg/Teff ratio). n=6 for UVB-irradiated mice, n=9 for nonirradiated mice, and n=4 for sham mice. B, The expression levels of Treg-associated markers were analyzed gating on $CD4^+Foxp3^+$ Tregs in spleen. n=6 to 9 mice per group. C, Lymphoid cells from spleen were stimulated with phorbol 12-myristate 13-acetate and ionomycin in vitro. Intracellular cytokine staining was performed. The graphs represent the frequencies of IFN-γ^+, IL-4^+, IL-10^+, and IL-17^+ $CD4^+$ T cells in the spleen of UVB-irradiated or control mice. The ratio of IFN-γ^+ $CD4^+$ T cells to IL-4^+ $CD4^+$ T cells was determined as T helper type 1 (Th1)/Th2 ratio. n=6 to 9 mice per group. D, Representative results of CD44 and CD62L expression in para-aortic LN $CD4^+$ T cells assessed by flow cytometry. The graph represents the percentage of $CD44^{high}CD62L^{low}$ Teffs within the $CD4^+$ population. n=6 to 8 mice per group. Mean values±SEM are plotted in (A through D). *P<0.05, **P<0.01, ***P<0.001. LN, lymph node; MFI, mean fluorescence intensity; UVB, ultraviolet B.

of $CD4^+Foxp3^+$ Tregs was abrogated in Treg-depleted DEREG/*Apoe*$^{-/-}$ mice (Figure S4B and S4C). Next, we examined the effect of UVB irradiation on AAA development under Treg-depleted conditions. Twelve-week-old DEREG/*Apoe*$^{-/-}$ mice fed a high-cholesterol diet were infused with angiotensin II by osmotic pumps, injected with diphtheria toxin for 2 consecutive days before implanting osmotic pumps and once weekly thereafter for 4 weeks, and euthanized at 16 weeks of age for evaluation of AAA formation (Figure 5A). There were no significant differences in body weight and plasma lipid profile between UVB-irradiated and nonirradiated mice under Treg-depleted conditions (Table 2). We found that UVB-

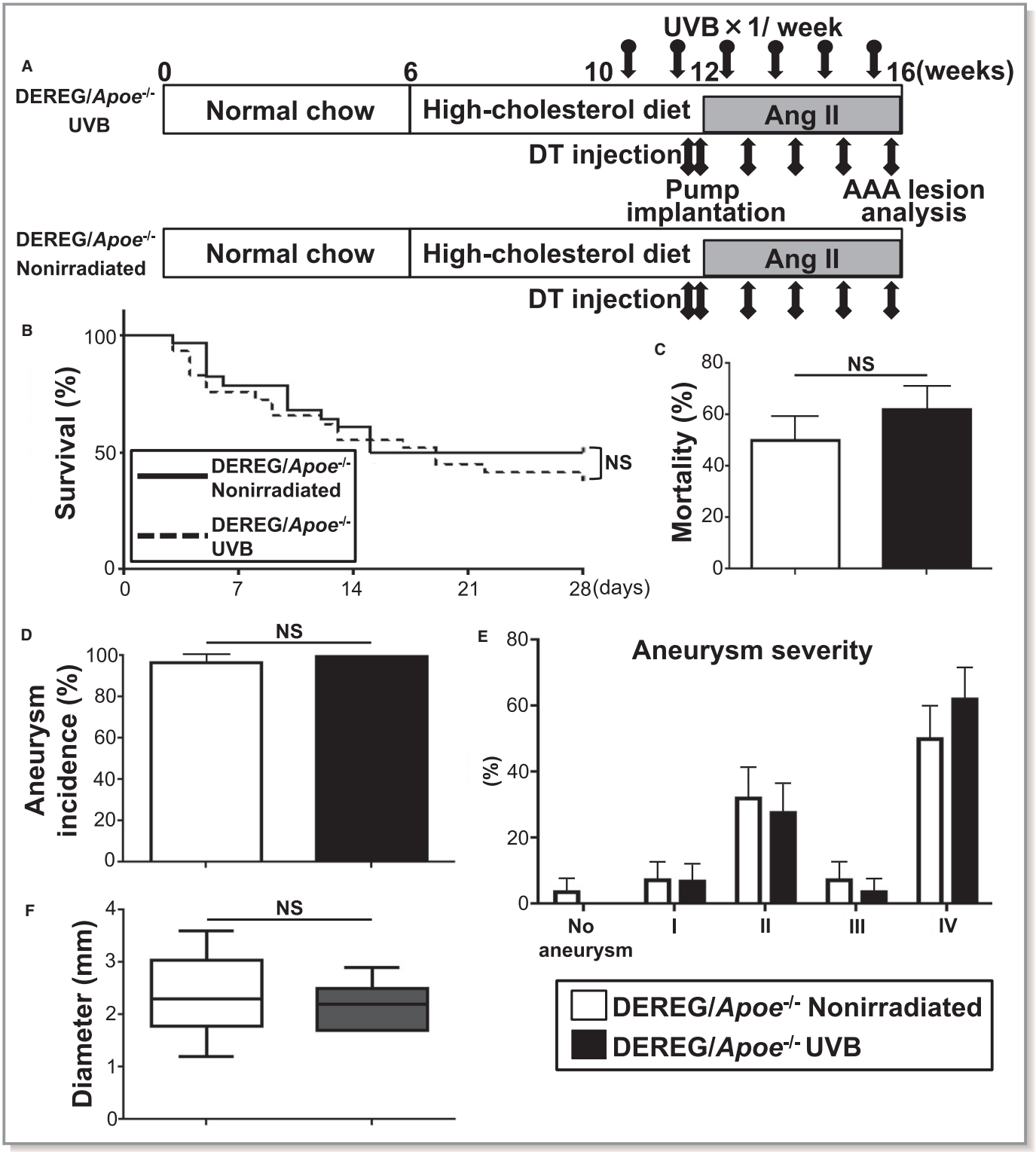

Figure 5. UVB-induced $CD4^+Foxp3^+$ regulatory T cells play a critical role in limiting the development of Ang II–induced AAA. A, Experimental design. Arrows with circle represent 5 kJ/m^2 UVB irradiation. Arrows with square represent intraperitoneal injection with 1.0 μg of DT. B, Survival rate in UVB-irradiated (n=29) and nonirradiated (n=28) DEREG/apolipoprotein E–deficient (DEREG/*Apoe*$^{-/-}$) mice. C, Mortality rate of AAA in UVB-irradiated (n=29) and nonirradiated (n=28) DEREG/*Apoe*$^{-/-}$ mice. D, Incidence of AAA in UVB-irradiated (n=29) and nonirradiated (n=28) DEREG/*Apoe*$^{-/-}$ mice. E, Severity of aneurysm in UVB-irradiated (n=11) and nonirradiated (n=14) DEREG/*Apoe*$^{-/-}$ mice. Error bars represent standard error in (C through E). F, Maximal diameter of abdominal aorta in UVB-irradiated (n=11) and nonirradiated (n=14) DEREG/*Apoe*$^{-/-}$ mice. In the box-and-whisker plot, middle line represents median value, box indicates interquartile range (25th–75th percentiles), and range bars show maximum and minimum. AAA indicates abdominal aortic aneurysm; Ang II, angiotensin II; DT, diphtheria toxin; NS, not significant; UVB, ultraviolet B.

Table 2. Body Weight, SBP, and Plasma Lipid Profile in 16-Week-Old UVB-Irradiated and Nonirradiated DEREG/Apolipoprotein E–Deficient Mice

Parameters	Nonirradiated	UVB
Body weight, g	24.0±0.9 (n=14)	25.8±0.9 (n=11)
SBP (before), mm Hg	101.5±1.5 (n=14)	102.1±1.5 (n=11)
SBP (after), mm Hg	137.5±2.9* (n=14)	131.9±3.0* (n=11)
Total cholesterol, mg/dL	774.0 (666.0–1160.0) (n=11)	1050.0 (861.0–1240.0) (n=11)
HDL cholesterol, mg/dL	15.0 (9.0–21.0) (n=11)	15.0 (12.5–19.5) (n=9)
Triglycerides, mg/dL	44.0 (23.0–65.0) (n=11)	27.0 (17.5–33.0) (n=9)

Data are expressed as mean±SEM or median (25–75% quartiles). HDL indicates high-density lipoprotein SBP, systolic blood pressure; SBP (before), SBP before angiotensin II infusion; SBP (after), SBP after angiotensin II infusion for 4 weeks; UVB, ultraviolet B. *P<0.05 vs SBP (before) in the same group. There are no statistically significant differences in all parameters between UVB-irradiated and nonirradiated mice.

dependent decrease in the incidence and mortality of AAA was abrogated in Treg-depleted DEREG/*Apoe*$^{-/-}$ mice (Figure 5B through 5D). Moreover, UVB irradiation did not affect the severity and diameter of the abdominal aneurysm under Treg-depleted conditions (Figure 5E and 5F). Immunohistochemical studies of the aneurysmal lesions in aorta revealed that UVB-dependent protective effects such as decreased accumulation of macrophages and CD4$^+$ T cells were abrogated on Treg depletion (Figure S5A and S5B). In addition, we observed no increase in the number of Tregs and the Treg/CD4$^+$ T cell ratio within the aneurysmal lesions of UVB-irradiated mice under Treg-depleted conditions (Figure S5B and S5C). These data provide direct evidence that UVB-induced CD4$^+$Foxp3$^+$ Tregs play a critical role in limiting aortic inflammation and AAA development.

Discussion

Immunoinflammatory reactions in the arterial wall have been shown to be a critical mechanism shared between AAA and atherosclerotic disease; however, effective medical therapies against AAA that could intervene in inflammation or the immune system currently do not exist, and surgery is considered a standard treatment. In the present study, we investigated the effect of UVB irradiation on AAA formation and its underlying mechanisms in angiotensin II–infused hypercholesterolemic mice. We demonstrated that UVB irradiation inhibited the development of angiotensin II–induced AAA and reduced mortality under hypercholesterolemic conditions. The protective effects of this therapy were associated with a marked reduction in the accumulation of macrophages and CD4$^+$ T cells in the aortic aneurysm tissue, along with systemic expansion of CD4$^+$Foxp3$^+$ Tregs and decreased number of CD4$^+$CD44^{high}CD62L^{low} Teffs in para-aortic LNs. Experimental studies in Treg-depleted mice clearly demonstrated that UVB-induced CD4$^+$Foxp3$^+$ Tregs played a critical role in limiting aortic inflammation and AAA development. Our data suggest that UVB irradiation may be a novel therapeutic approach for preventing AAA.

The potential relevance of sunlight exposure to risk of cardiovascular disease has been suggested in several epidemiological studies and may be attributable to low vitamin D levels.[32–34] Because cutaneous synthesis of vitamin D is dominant compared with dietary intake, inadequate sunlight exposure causes vitamin D deficiency.[35] Notably, recent epidemiological studies have highlighted the increasing prevalence of vitamin D deficiency and its association with increased risks of AAA.[36,37] These reports raise the possibility that UVB-dependent promotion of cutaneous synthesis of vitamin D may be responsible for attenuation of AAA formation in the present study. Whereas our recent work showed a significant increase in biologically active 1,25-dihydroxyvitamin D plasma levels in UVB-irradiated *Apoe*$^{-/-}$ mice without angiotensin II infusion,[25] we found no changes in its plasma levels in the present study in UVB-irradiated *Apoe*$^{-/-}$ mice treated with angiotensin II, excluding a substantial contribution of vitamin D to the protective effects of UVB irradiation in our AAA model. Angiotensin II is reported to downregulate renal Klotho expression,[38] which leads to increased levels of fibroblast growth factor 23; subsequent suppression of 1α-hydroxylase, known to convert circulating storage form 25-hydroxyvitamin D to highly active 1,25-dihydroxyvitamin D; and reduced production of 1,25-dihydroxyvitamin D in the kidney.[39] Consequently, we speculate that the inconsistency in plasma 1,25-dihydroxyvitamin D levels between the present study and previous work[25] may be due to downregulation of renal Klotho expression in this angiotensin II–induced AAA model. We propose a novel vitamin D–independent mechanism for UVB-dependent prevention of AAA, attributed to the modification of the immune system.

It is recognized that innate and adaptive immunity are deeply involved in the pathogenesis of AAA. Although aortic inflammation via Th-mediated immune responses is thought to accelerate the development of AAA,[4] the role of each subset including the Th1, Th2, and Th17 lineage in AAA remains to be elucidated. Because many differences in Th immune responses such as Th1/Th2 balance can be seen between atherosclerotic disease and AAA, modulation of only these responses does not seem to be effective for preventing both diseases. Experimental and clinical studies have demonstrated that the imbalance between pathogenic Teffs and Tregs may be critical for the pathogenesis of AAA. It has been shown that therapeutic intervention aimed at shifting the Treg/Teff balance toward Tregs represents a possible

therapeutic approach against both atherosclerotic disease[26,40–42] and AAA.[16–18] We recently reported that selective expansion of active $CD4^+Foxp3^+$ Tregs by injection of a recombinant mouse IL-2/anti–IL-2 monoclonal antibody complex led to protection against AAA formation in angiotensin II–infused *Apoe*$^{-/-}$ mice without affecting the Th1/Th2 balance,[17] suggesting a possible therapeutic approach to prevent AAA. Although such pharmacological therapy is effective and does not cause severe side effects in mouse disease models, antibody- or cytokine-based therapies could activate excessive immune responses in clinical settings. To achieve clinical application, other strategies that selectively augment Treg function but do not evoke inflammatory responses should be developed.

In addition to pharmacological approaches, transfer of Tregs has been shown to reduce AAA development in angiotensin II–infused *Apoe*$^{-/-}$ mice.[16,18] There are clinical studies in which transfer of ex vivo expanded Tregs was performed for the treatment of autoimmune disease or graft-versus-host disease after bone marrow transplantation; however, indication of such cell-based therapy is now quite limited because separation of high amounts of pure Tregs is technically difficult. In this study, we demonstrated that UVB irradiation shifted the Treg/Teff balance toward Tregs without affecting the systemic Th1/Th2 balance, which resulted in the prevention of the development of angiotensin II–induced AAA. Importantly, in clinical settings, UV-based phototherapy is safe and effective for immunoinflammatory cutaneous diseases such as psoriasis, atopic dermatitis, and cutaneous T-cell lymphoma. Notably, in recent clinical studies, UVB phototherapy was shown to expand $CD4^+CD25^+Foxp3^+$ Tregs in the peripheral blood, which is associated with reduced disease activity.[43,44] These reports support the idea that UVB phototherapy might be beneficial in treating human AAA through expansion of $CD4^+Foxp3^+$ Tregs, although the role of Tregs in human AAA remains to be explored. Although careful management is required for application in clinical settings, a certain degree of UVB irradiation may be beneficial for preventing human AAA, if skin condition is checked regularly by a dermatologist.

Tregs are known to have constitutively high expression of the CD25 molecule, and activated Teffs also show high expression levels of this molecule.[45] Foxp3 is considered to be the most reliable molecular marker for Tregs and a master regulator of their development and function.[45] We recently established a novel mouse model (DEREG/*Apoe*$^{-/-}$ mice) in which diphtheria toxin injection leads to selective and efficient depletion of $CD4^+Foxp3^+$ Tregs under hypercholesterolemic conditions.[17] In our previous work using the same mouse model, we evaluated the exact effect of endogenous $CD4^+Foxp3^+$ Treg deficiency on AAA formation and demonstrated that endogenous $CD4^+Foxp3^+$ Tregs play a protective role against AAA by dampening immunoinflammatory responses.[17] In the present study, to directly investigate the contribution of systemic $CD4^+Foxp3^+$ Tregs to AAA prevention following UVB exposure, we treated DEREG/*Apoe*$^{-/-}$ mice with angiotensin II and diphtheria toxin to induce AAA formation under Treg-depleted conditions. Our data on these mice clearly demonstrated that UVB-induced expansion of $CD4^+Foxp3^+$ Tregs play an essential role in regulating pathogenic immunoinflammatory responses and the development of AAA. Because AAA patients have high incidence of atherosclerotic disease and UVB exposure inhibits the development and progression of atherosclerosis,[25] these results suggest that a novel immunomodulatory approach such as UVB-based phototherapy may be effective for preventing both AAA and atherosclerosis through enhancing Treg-mediated immune responses. Elucidation of detailed molecular mechanisms for UVB-dependent Treg induction and suppression of AAA development will help us develop effective therapies for AAA.

In conclusion, we provide evidence that UVB irradiation reduces the development and related mortality of angiotensin II–induced AAA in hypercholesterolemic mice and that these protective effects are associated with reduced inflammatory responses in aortic aneurysmal lesions, possibly due to a shift of the Treg/Teff balance toward Tregs. These findings should be applied cautiously in clinical situations; however, based on the chronic immunoinflammatory nature and protective effects of UVB exposure shared by AAA and atherosclerotic disease, our data suggest that UVB-mediated modulation of immunoinflammatory reactions could be an attractive noninvasive approach to preventing not only atherosclerotic disease but also AAA.

Acknowledgments

We would like to thank Satomi Minami for technical assistance. DEREG mice were a generous gift from Dr. Tim Sparwasser (Institute of Infection Immunology, Twincore, Centre for Experimental and Clinical Infection Research).

Sources of Funding

This work was supported by JSPS KAKENHI Grant Number 25860601 (Sasaki), 15K09156 (Sasaki), and 16K09516 (Yamashita), and research grants from Banyu Life Science Foundation International (Sasaki), Takeda Scientific Foundation (Sasaki), and The Japan Circulation Society Translational Research Foundation (Hirata).

Disclosures

None.

References

1. Golledge J, Muller J, Daugherty A, Norman P. Abdominal aortic aneurysm: pathogenesis and implications for management. *Arterioscler Thromb Vasc Biol*. 2006;26:2605–2613.
2. Kuivaniemi H, Platsoucas CD, Tilson MD III. Aortic aneurysms: an immune disease with a strong genetic component. *Circulation*. 2008;117:242–252.
3. Golledge J, Norman PE. Current status of medical management for abdominal aortic aneurysm. *Atherosclerosis*. 2011;217:57–63.
4. Dale MA, Ruhlman MK, Baxter BT. Inflammatory cell phenotypes in AAAs: their role and potential as targets for therapy. *Arterioscler Thromb Vasc Biol*. 2015;35:1746–1755.
5. Shimizu K, Mitchell RN, Libby P. Inflammation and cellular immune responses in abdominal aortic aneurysms. *Arterioscler Thromb Vasc Biol*. 2006;26:987–994.
6. Shimizu K, Shichiri M, Libby P, Lee RT, Mitchell RN. Th2-predominant inflammation and blockade of IFN-gamma signaling induce aneurysms in allografted aortas. *J Clin Invest*. 2004;114:300–308.
7. Schonbeck U, Sukhova GK, Gerdes N, Libby P. T(H)2 predominant immune responses prevail in human abdominal aortic aneurysm. *Am J Pathol*. 2002;161:499–506.
8. Gupta S, Pablo AM, Jiang X, Wang N, Tall AR, Schindler C. IFN-gamma potentiates atherosclerosis in ApoE knock-out mice. *J Clin Invest*. 1997;99:2752–2761.
9. King VL, Lin AY, Kristo F, Anderson TJ, Ahluwalia N, Hardy GJ, Owens AP III, Howatt DA, Shen D, Tager AM, Luster AD, Daugherty A, Gerszten RE. Interferon-gamma and the interferon-inducible chemokine CXCL10 protect against aneurysm formation and rupture. *Circulation*. 2009;119:426–435.
10. Xiong W, Zhao Y, Prall A, Greiner TC, Baxter BT. Key roles of CD4+ T cells and IFN-gamma in the development of abdominal aortic aneurysms in a murine model. *J Immunol*. 2004;172:2607–2612.
11. Galle C, Schandene L, Stordeur P, Peignois Y, Ferreira J, Wautrecht JC, Dereume JP, Goldman M. Predominance of type 1 CD4+ T cells in human abdominal aortic aneurysm. *Clin Exp Immunol*. 2005;142:519–527.
12. Ait-Oufella H, Salomon BL, Potteaux S, Robertson AK, Gourdy P, Zoll J, Merval R, Esposito B, Cohen JL, Fisson S, Flavell RA, Hansson GK, Klatzmann D, Tedgui A, Mallat Z. Natural regulatory T cells control the development of atherosclerosis in mice. *Nat Med*. 2006;12:178–180.
13. Klingenberg R, Gerdes N, Badeau RM, Gistera A, Strodthoff D, Ketelhuth DF, Lundberg AM, Rudling M, Nilsson SK, Olivecrona G, Zoller S, Lohmann C, Luscher TF, Jauhiainen M, Sparwasser T, Hansson GK. Depletion of FOXP3+ regulatory T cells promotes hypercholesterolemia and atherosclerosis. *J Clin Invest*. 2013;123:1323–1334.
14. Sasaki N, Yamashita T, Kasahara K, Takeda M, Hirata K. Regulatory T cells and tolerogenic dendritic cells as critical immune modulators in atherogenesis. *Curr Pharm Des*. 2015;21:1107–1117.
15. Ait-Oufella H, Wang Y, Herbin O, Bourcier S, Potteaux S, Joffre J, Loyer X, Ponnuswamy P, Esposito B, Dalloz M, Laurans L, Tedgui A, Mallat Z. Natural regulatory T cells limit angiotensin II-induced aneurysm formation and rupture in mice. *Arterioscler Thromb Vasc Biol*. 2013;33:2374–2379.
16. Meng X, Yang J, Zhang K, An G, Kong J, Jiang F, Zhang Y, Zhang C. Regulatory T cells prevent angiotensin II-induced abdominal aortic aneurysm in apolipoprotein E knockout mice. *Hypertension*. 2014;64:875–882.
17. Yodoi K, Yamashita T, Sasaki N, Kasahara K, Emoto T, Matsumoto T, Kita T, Sasaki Y, Mizoguchi T, Sparwasser T, Hirata K. Foxp3+ regulatory T cells play a protective role in angiotensin II-induced aortic aneurysm formation in mice. *Hypertension*. 2015;65:889–895.
18. Zhou Y, Wu W, Lindholt JS, Sukhova GK, Libby P, Yu X, Shi GP. Regulatory T cells in human and angiotensin II-induced mouse abdominal aortic aneurysms. *Cardiovasc Res*. 2015;107:98–107.
19. Yin M, Zhang J, Wang Y, Wang S, Bockler D, Duan Z, Xin S. Deficient CD4+CD25+ T regulatory cell function in patients with abdominal aortic aneurysms. *Arterioscler Thromb Vasc Biol*. 2010;30:1825–1831.
20. Dinh TN, Kyaw TS, Kanellakis P, To K, Tipping P, Toh BH, Bobik A, Agrotis A. Cytokine therapy with interleukin-2/anti-interleukin-2 monoclonal antibody complexes expands CD4+CD25+Foxp3+ regulatory T cells and attenuates development and progression of atherosclerosis. *Circulation*. 2012;126:1256–1266.
21. Schwarz T. Mechanisms of UV-induced immunosuppression. *Keio J Med*. 2005;54:165–171.
22. Araneo BA, Dowell T, Moon HB, Daynes RA. Regulation of murine lymphokine production in vivo. Ultraviolet radiation exposure depresses IL-2 and enhances IL-4 production by T cells through an IL-1-dependent mechanism. *J Immunol*. 1989;143:1737–1744.
23. Shreedhar VK, Pride MW, Sun Y, Kripke ML, Strickland FM. Origin and characteristics of ultraviolet-B radiation-induced suppressor T lymphocytes. *J Immunol*. 1998;161:1327–1335.
24. Van Loveren H, Boonstra A, Van Dijk M, Fluitman A, Savelkoul HF, Garssen J. UV exposure alters respiratory allergic responses in mice. *Photochem Photobiol*. 2000;72:253–259.
25. Sasaki N, Yamashita T, Kasahara K, Fukunaga A, Yamaguchi T, Emoto T, Yodoi K, Matsumoto T, Nakajima K, Kita T, Takeda M, Mizoguchi T, Hayashi T, Sasaki Y, Hatakeyama M, Taguchi K, Washio K, Sakaguchi S, Malissen B, Nishigori C, Hirata KI. UVB exposure prevents atherosclerosis by regulating immunoinflammatory responses. *Arterioscler Thromb Vasc Biol*. 2017;37:66–74.
26. Sasaki N, Yamashita T, Takeda M, Shinohara M, Nakajima K, Tawa H, Usui T, Hirata K. Oral anti-CD3 antibody treatment induces regulatory T cells and inhibits the development of atherosclerosis in mice. *Circulation*. 2009;120:1996–2005.
27. Daugherty A, Manning MW, Cassis LA. Angiotensin II promotes atherosclerotic lesions and aneurysms in apolipoprotein E-deficient mice. *J Clin Invest*. 2000;105:1605–1612.
28. Kunisada M, Kumimoto H, Ishizaki K, Sakumi K, Nakabeppu Y, Nishigori C. Narrow-band UVB induces more carcinogenic skin tumors than broad-band UVB through the formation of cyclobutane pyrimidine dimer. *J Invest Dermatol*. 2007;127:2865–2871.
29. Nakajima H, Ishida T, Satomi-Kobayashi S, Mori K, Hara T, Sasaki N, Yasuda T, Toh R, Tanaka H, Kawai H, Hirata K. Endothelial lipase modulates pressure overload-induced heart failure through alternative pathway for fatty acid uptake. *Hypertension*. 2013;61:1002–1007.
30. Takeda M, Yamashita T, Sasaki N, Nakajima K, Kita T, Shinohara M, Ishida T, Hirata K. Oral administration of an active form of vitamin D3 (calcitriol) decreases atherosclerosis in mice by inducing regulatory T cells and immature dendritic cells with tolerogenic functions. *Arterioscler Thromb Vasc Biol*. 2010;30:2495–2503.
31. Lahl K, Loddenkemper C, Drouin C, Freyer J, Arnason J, Eberl G, Hamann A, Wagner H, Huehn J, Sparwasser T. Selective depletion of Foxp3+ regulatory T cells induces a scurfy-like disease. *J Exp Med*. 2007;204:57–63.
32. Voors AW, Johnson WD. Altitude and arteriosclerotic heart disease mortality in white residents of 99 of the 100 largest cities in the United States. *J Chronic Dis*. 1979;32:157–162.
33. Scragg R. Seasonality of cardiovascular disease mortality and the possible protective effect of ultra-violet radiation. *Int J Epidemiol*. 1981;10:337–341.
34. Grimes DS, Hindle E, Dyer T. Sunlight, cholesterol and coronary heart disease. *QJM*. 1996;89:579–589.
35. Holick MF. Vitamin D deficiency. *N Engl J Med*. 2007;357:266–281.
36. Hultgren R, Forsberg J, Alfredsson L, Swedenborg J, Leander K. Regional variation in the incidence of abdominal aortic aneurysm in Sweden. *Br J Surg*. 2012;99:647–653.
37. Sampson UK, Norman PE, Fowkes FG, Aboyans V, Song Y, Harrell FE Jr, Forouzanfar MH, Naghavi M, Denenberg JO, McDermott MM, Criqui MH, Mensah GA, Ezzati M, Murray C. Estimation of global and regional incidence and prevalence of abdominal aortic aneurysms 1990 to 2010. *Glob Heart*. 2014;9:159–170.
38. Mitani H, Ishizaka N, Aizawa T, Ohno M, Usui S, Suzuki T, Amaki T, Mori I, Nakamura Y, Sato M, Nangaku M, Hirata Y, Nagai R. In vivo klotho gene transfer ameliorates angiotensin II-induced renal damage. *Hypertension*. 2002;39:838–843.
39. Shroff R, Wan M, Rees L. Can vitamin D slow down the progression of chronic kidney disease? *Pediatr Nephrol*. 2012;27:2167–2173.
40. Kita T, Yamashita T, Sasaki N, Kasahara K, Sasaki Y, Yodoi K, Takeda M, Nakajima K, Hirata K. Regression of atherosclerosis with anti-CD3 antibody via augmenting a regulatory T-cell response in mice. *Cardiovasc Res*. 2014;102:107–117.
41. Kasahara K, Sasaki N, Yamashita T, Kita T, Yodoi K, Sasaki Y, Takeda M, Hirata K. CD3 antibody and IL-2 complex combination therapy inhibits atherosclerosis by augmenting a regulatory immune response. *J Am Heart Assoc*. 2014;3:e000719. DOI: 10.1161/JAHA.113.000719.
42. Matsumoto T, Sasaki N, Yamashita T, Emoto T, Kasahara K, Mizoguchi T, Hayashi T, Yodoi K, Kitano N, Saito T, Yamaguchi T, Hirata K. Overexpression of cytotoxic T-lymphocyte-associated antigen-4 prevents atherosclerosis in mice. *Arterioscler Thromb Vasc Biol*. 2016;36:1141–1151.
43. Furuhashi T, Saito C, Torii K, Nishida E, Yamazaki S, Morita A. Photo(chemo) therapy reduces circulating Th17 cells and restores circulating regulatory T cells in psoriasis. *PLoS One*. 2013;8:e54895.
44. Iyama S, Murase K, Sato T, Hashimoto A, Tatekoshi A, Horiguchi H, Kamihara Y, Ono K, Kikuchi S, Takada K, Kawano Y, Hayashi T, Miyanishi K, Sato Y, Takimoto R, Kobune M, Mori S, Kato J, Yamashita T, Kato J. Narrowband ultraviolet B phototherapy ameliorates acute graft-versus-host disease by a mechanism involving in vivo expansion of CD4+CD25+Foxp3+ regulatory T cells. *Int J Hematol*. 2014;99:471–476.
45. Sakaguchi S, Yamaguchi T, Nomura T, Ono M. Regulatory T cells and immune tolerance. *Cell*. 2008;133:775–787.

SUPPLEMENTAL MATERIAL

Figure S1

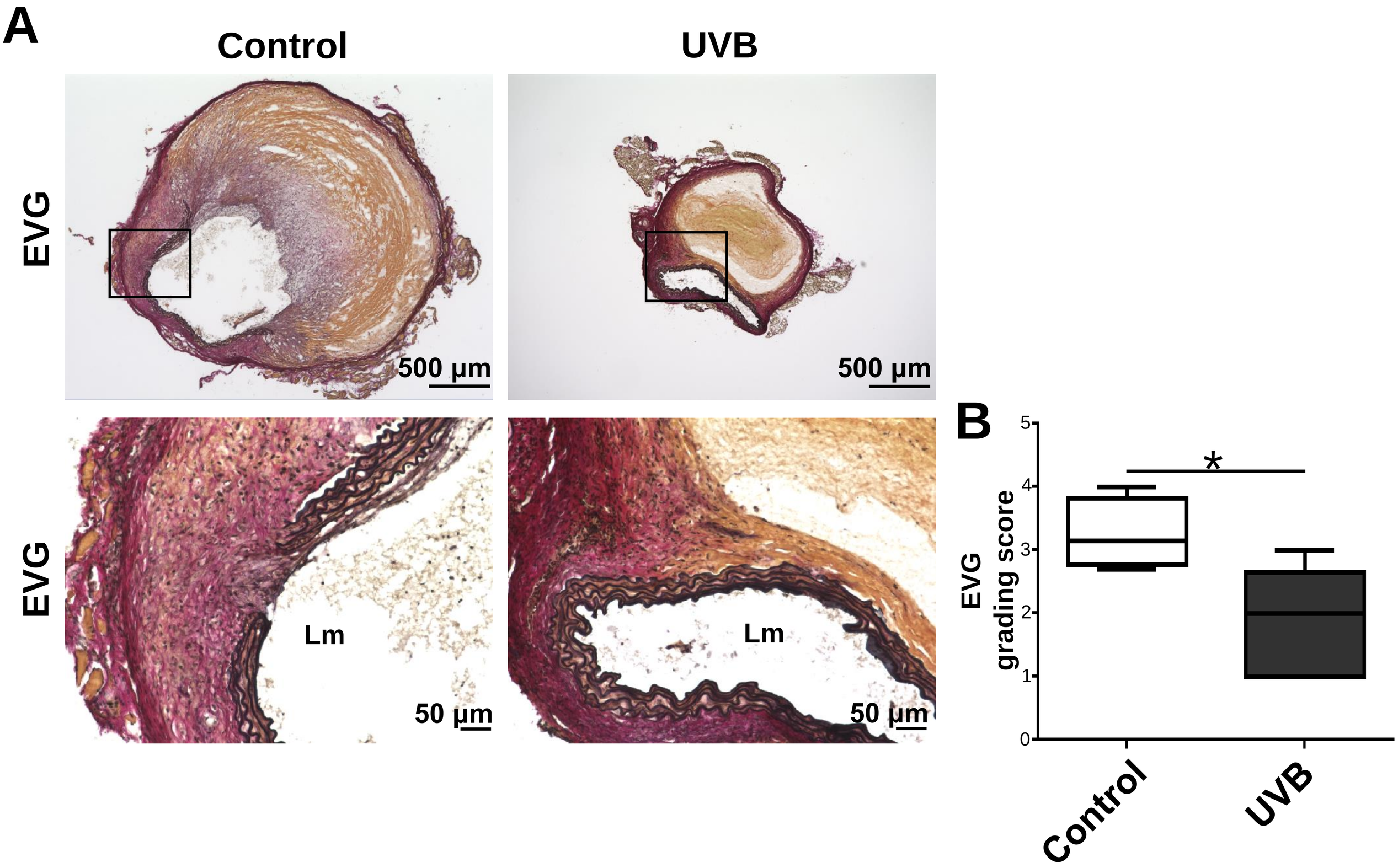

Figure S1. Effects of UVB irradiation on elastin degradation in aneurysmal lesions. A and B, Representative photomicrographs (A) and categorical score (B) of elastin degradation in the aneurysmal lesions of UVB-irradiated (n=5) and nonirradiated (n=4) mice. Boxed area is expanded to show representative high-power fields in serial sections. Scale bar, as shown in figures. Lm indicates lumen. In the box-and-whisker plot shown in (B), middle line represents median value, box indicates interquartile range (25th-75th percentiles), and range bars show maximum and minimum. *P<0.05.

Figure S2

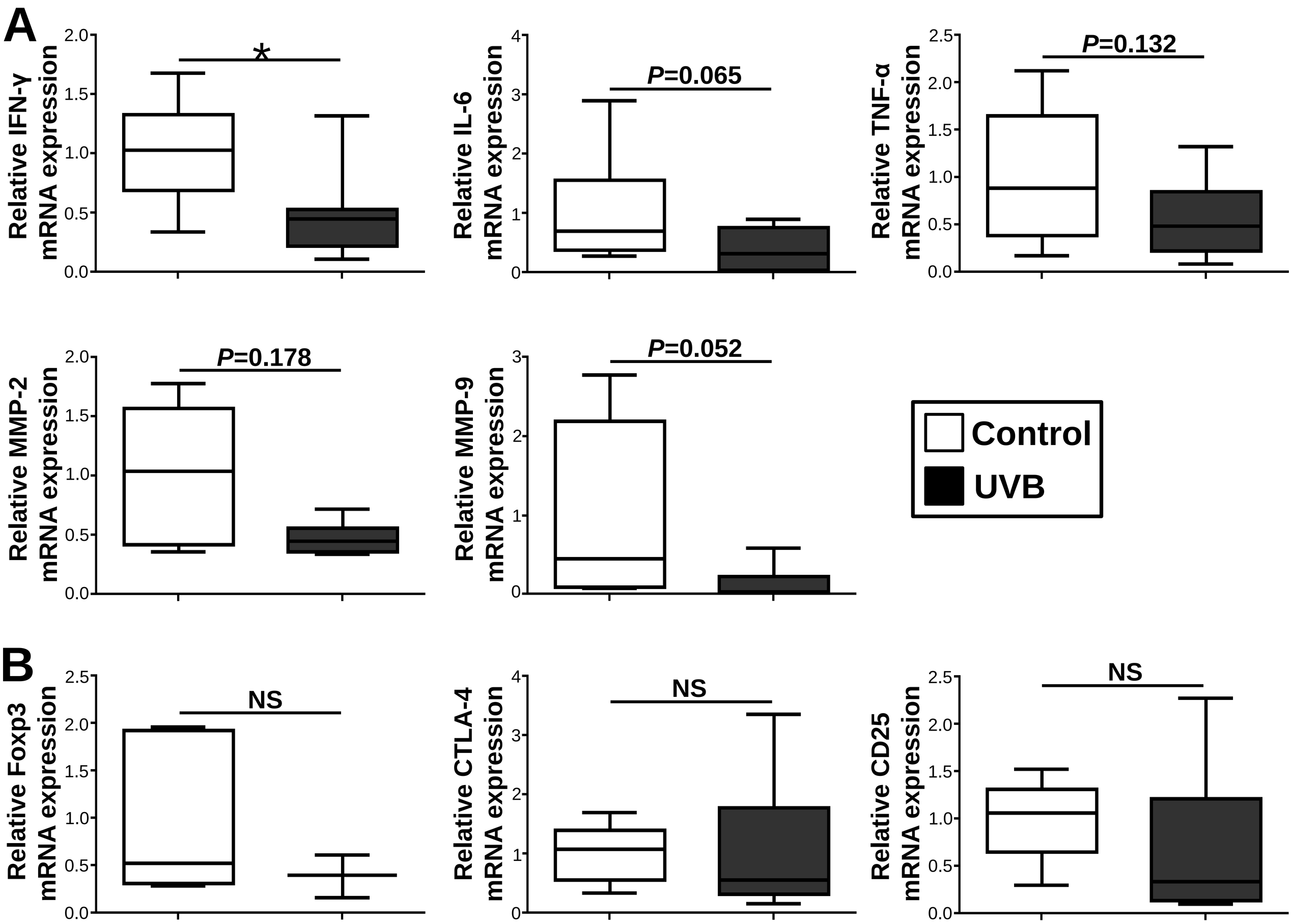

Figure S2. UVB irradiation reduces inflammation in the aneurysmal tissues. Total RNA was extracted from the supra-renal aortas of 13-week-old UVB-irradiated or nonirradiated mice infused with angiotensin II. Messenger RNA expressions of proinflammatory cytokines (interferon (IFN)-γ, interleukin (IL)-6, tumor necrosis factor (TNF)-α, n=9 to 10 mice per group), matrix mettaloproteinases (MMPs) (MMP-2, MMP-9, n=5 to 6 mice per group) (A), and Treg-associated molecules (forkhead box P3 (Foxp3), cytotoxic T lymphocyte-associated antigen-4 (CTLA-4), CD25, n=3 to 6 mice per group) (B) were quantified by quantitative real-time reverse transcription PCR and normalized to GAPDH. In the box-and-whisker plot, middle line represents median value, box indicates interquartile range (25th-75th percentiles), and range bars show maximum and minimum. $^{*}P<0.05$.

Figure S3

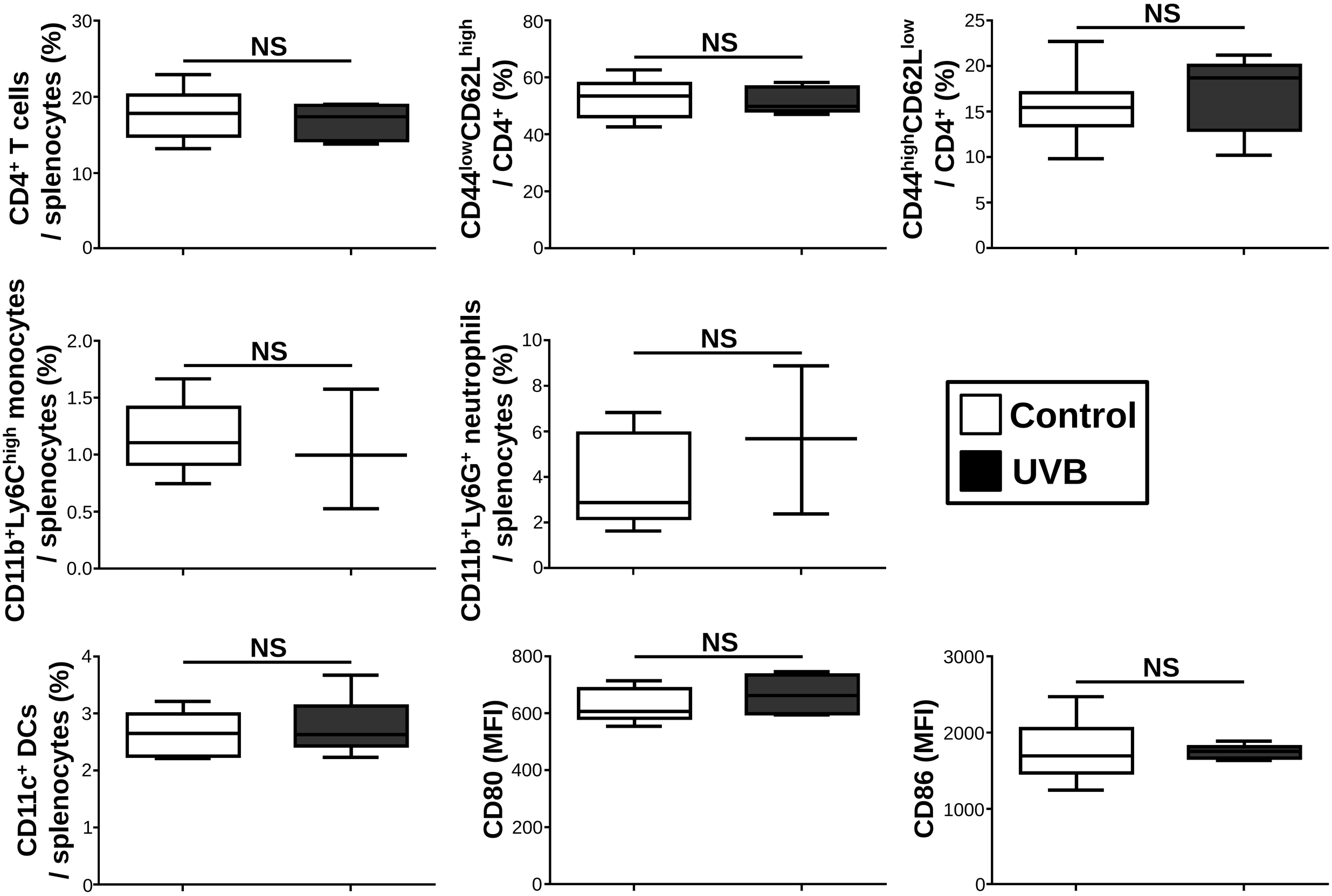

Figure S3. Effects of UVB irradiation on immune cells other than $CD4^+$forkhead box $P3^+$ regulatory T cells (Tregs) in the spleen. Apolipoprotein E-deficient mice were irradiated with 5 kJ/m^2 UVB once weekly for 3 weeks. Nonirradiated mice infused with angiotensin II served as controls. Seven days after the pump implantation and 4 days after the last UVB irradiation, lymphoid cells from spleen were prepared. Percentages of splenic $CD4^+$, naïve ($CD44^{low}CD62L^{high}$) and effector ($CD44^{high}CD62L^{low}$) T cells, $CD11b^+Ly6C^{high}$ monocyte, $CD11b^+Ly6G^+$ neutrophils, and $CD11c^+$ dendritic cells (DCs), and CD80 and CD86 expression on $CD11c^+$ DCs were determined by flow cytometry. NS indicates not significant; MFI, mean fluorescence intensity. n=3 to 9 mice per group. In the box-and-whisker plot, middle line represents median value, box indicates interquartile range (25th-75th percentiles), and range bars show maximum and minimum.

Figure S4

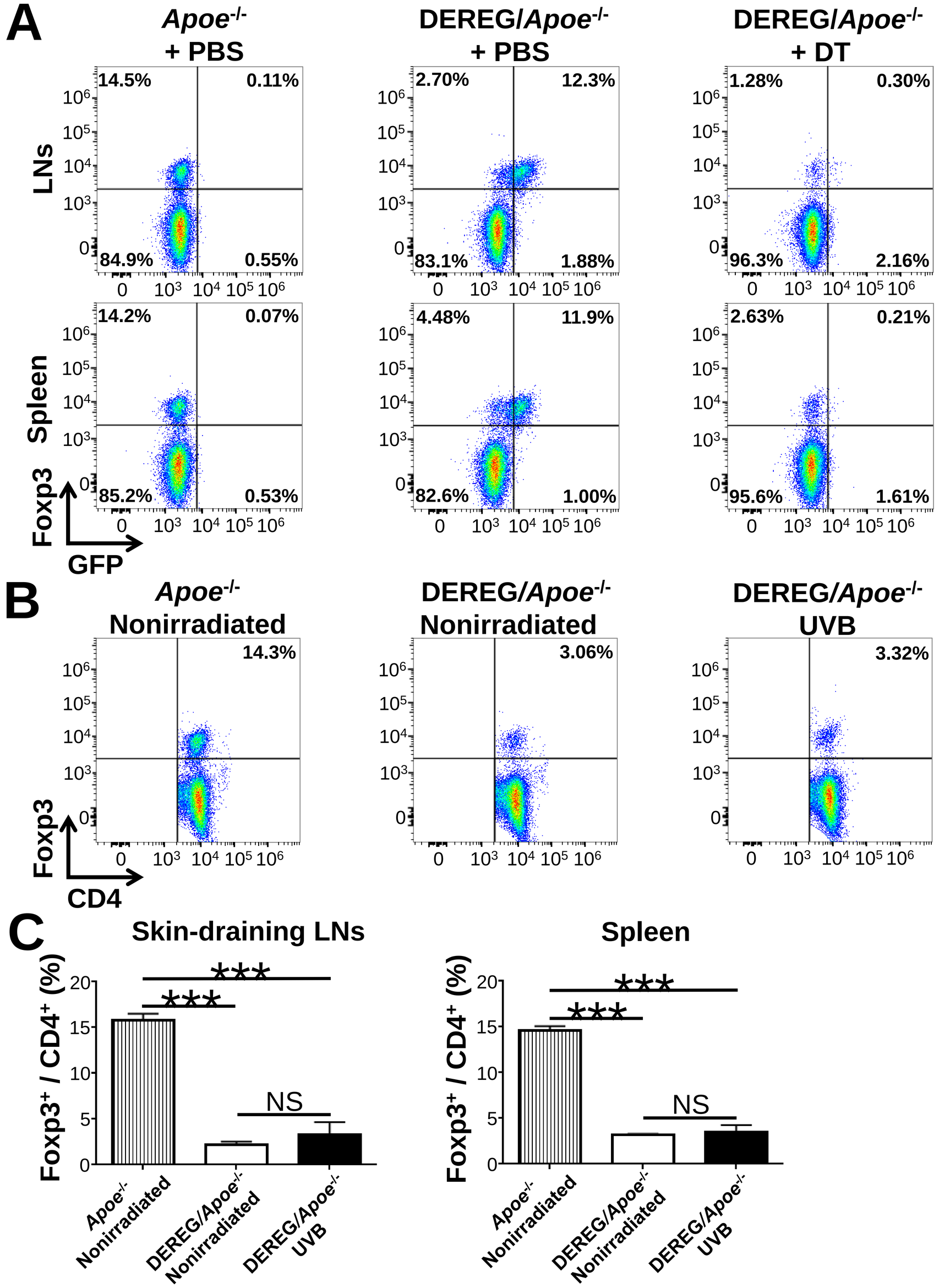

Figure S4. UVB-dependent expansion of CD4$^+$forkhead box P3 (Foxp3)$^+$ regulatory T cells (Tregs) could be abrogated in diphtheria toxin (DT)-treated DEREG/apolipoprotein E-deficient (*Apoe*$^{-/-}$) mice. A, The transgene encoding the diphtheria toxin receptor (DTR)-eGFP fusion protein, is expressed in CD4$^+$Foxp3$^+$ Tregs and is selectively depleted by DT injection. DEREG/*Apoe*$^{-/-}$ or *Apoe*$^{-/-}$ mice received daily intraperitoneal injections of DT (1μg/mouse) or PBS on consecutive days and were sacrificed 24 hours later after the second injection. Representative results of GFP and Foxp3 expression in skin-draining lymph node (LN) and splenic CD4$^+$ T cells assessed by flow cytometry. GFP, green fluorescent protein. B, C, DEREG/*Apoe*$^{-/-}$ mice were irradiated with 5 kJ/m^2 UVB once weekly for 2 weeks and received daily intraperitoneal injections of DT (1μg/mouse) on consecutive days. Nonirradiated DT-treated DEREG/*Apoe*$^{-/-}$ or PBS-treated *Apoe*$^{-/-}$ mice served as controls. Twenty-four hours after the second DT injection, lymphoid cells from skin-draining LNs and spleen were prepared. B, Representative results of Foxp3 expression in splenic CD4$^+$ T cells assessed by flow cytometry. C, The graphs represent the percentage of Foxp3$^+$ Tregs within the skin-draining LN and spleen CD4$^+$ population. NS indicates not significant. n=4 mice per group. Mean values ± sem are plotted. $^{***}P<0.001$.

Figure S5

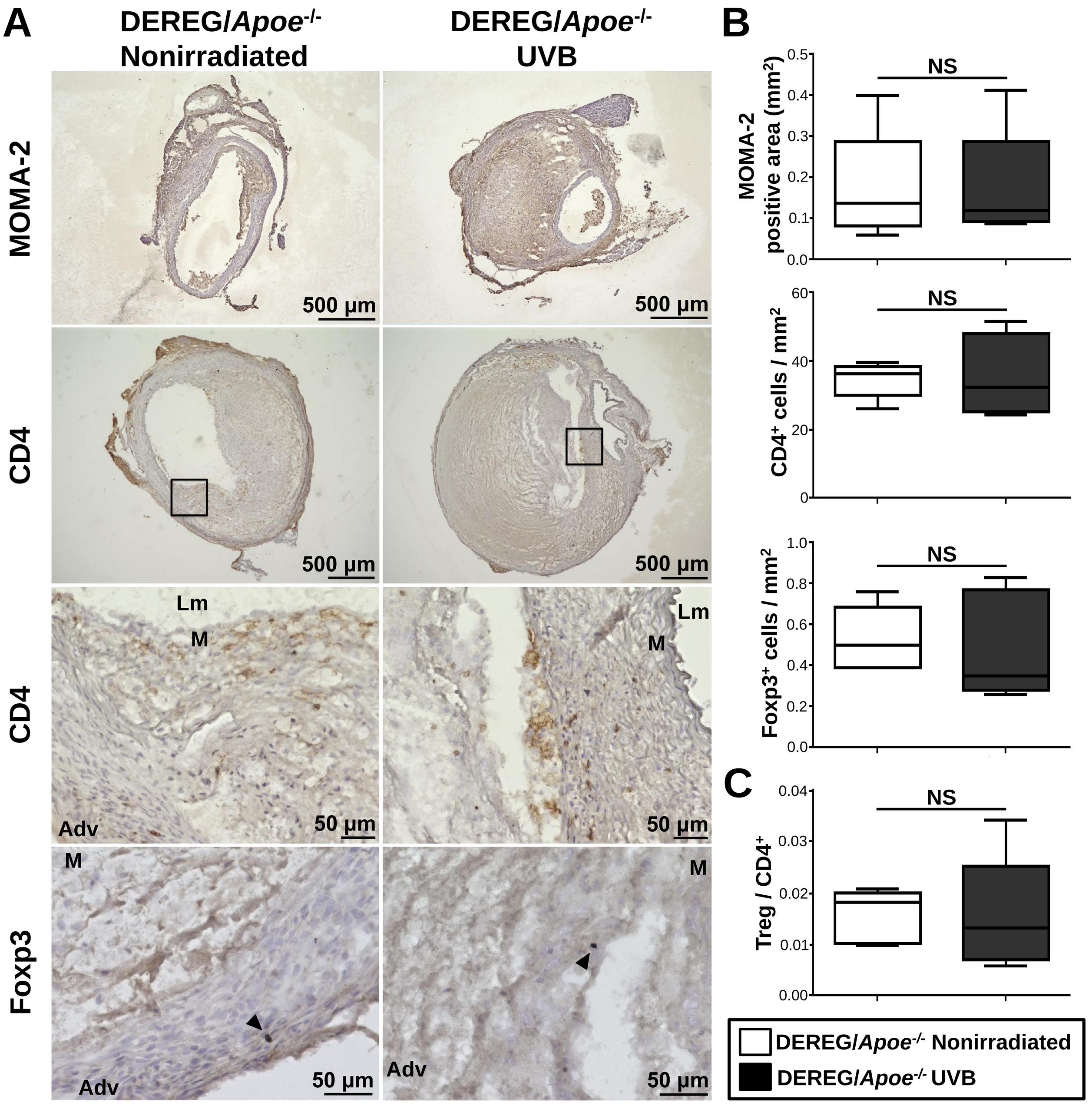

Figure S5. UVB-dependent protective effects such as decreased accumulation of macrophages and $CD4^+$ T cells were abrogated in diphtheria toxin (DT)-treated DEREG/apolipoprotein E-deficient (*Apoe*$^{-/-}$) mice. A, Representative photomicrographs of MOMA-2, CD4, and forkhead box P3 (Foxp3) staining in the abdominal aortic aneurysm lesions of UVB-irradiated and nonirradiated mice. Boxed area is expanded to show representative high-power fields in serial sections. Lm indicates lumen; M, media; Adv, adventitia. Arrowheads indicate $Foxp3^+$ cells. Scale bar, as shown in figures. B, Quantitative analyses of $MOMA\text{-}2^+$ macrophages, $CD4^+$ T cells, and $Foxp3^+$ regulatory T cells (Tregs) in the aneurysmal lesions in UVB-irradiated and nonirradiated mice. n=5 mice per group. C, The ratio of $Foxp3^+$ Tregs to $CD4^+$ T cells was determined (Treg/$CD4^+$ T cell ratio). In the box-and-whisker plot shown in (B) and (C), middle line represents median value, box indicates interquartile range (25th-75th percentiles), and range bars show maximum and minimum. NS indicates not significant.